A Theory that Connects Proton-Coupled Electron-Transfer and Hydrogen-Atom Transfer Reactions†

R. I. Cukier

Department of Chemistry, Michigan State University, East Lansing, Michigan 48824-1322

Received: June 25, 2001; In Final Form: October 12, 2001

A theory for proton-coupled electron-transfer (PCET) reactions (Cukier, R. I.; Nocera, D. *Ann. Rev. Phys. Chem*. **1998**, *49*, 337) is generalized to also apply to hydrogen-atom transfer (HAT) reactions. PCET was described as a concerted transfer of an electron and proton, with both species weakly coupled between their respective initial and final states, a nonadiabatic regime for both electron and proton. Here, we treat the electron adiabatically, asserting that it is strongly coupled and the proton can span the nonadiabatic to adiabatic regimes. A rate constant expression is obtained that incorporates the heavy-atom framework dynamics surrounding the transferring hydrogen atom as well as the effects of inner-sphere vibrational modes. Features of the rate constant that emerge are that modest isotope effects are often to be expected. The observation that some hydrogen-atom transfer reactions have small rate constants, small activation energies, and relatively small isotope effects can be understood on the basis of this theory. The contrasting kinetic properties between nitrogen and oxygen acids versus carbon acids can also be rationalized.

I. Introduction

The coupling between electron and proton transfer is an important pathway of charge transport in biological systems that has stimulated a great deal of theoretical[1−18] and experimental[19−36] interest. Electron-transfer (ET), proton-transfer (PT), proton-coupled electron-transfer (PCET), dissociative pcet (DPCET), and hydrogen-atom transfer (HAT) reactions have many features in common. They all occur by tunneling and, with the exception of hydrogen-atom transfer, typically involve large charge rearrangements with concomitant strong coupling to the surrounding medium. Deciding whether electron and proton transfer is a consecutive or a concerted process can be quite difficult, from both experimental and theoretical perspectives. Distinguishing between PCET and HAT also can be difficult.

An example of what we shall refer to as PCET is a step in the chain of charge-transfer reactions in the photosystem II oxygen-evolving complex (PSII/OEC), designated as Reaction 1 in Figure 1.[22,37−44] For a consecutive pathway, the reactions are

$$P680^+ + Y_ZOH{-}NR_2 \xrightarrow{ET} P680 + [Y_ZOH{-}NR_2]^{\bullet+} \xrightarrow{PT} P680 + [Y_ZO{-}HNR_2]^{\bullet+}$$

As a concerted process, the reaction is

$$P680^+ + Y_ZOH{-}NR_2 \xrightarrow{ETPT} P680 + [Y_ZO{-}HNR_2]^{\bullet+} \quad \text{(Scheme I)}$$

In this scheme, a reaction center chlorophyll P680 has been previously oxidized to $P680^+$. The tryrosine, denoted as Y_ZOH, is oxidized to a tryrosyl radical and re-reduces $P680^+$ to P680. The proton in the tyrosyl−histidine (NR_2) hydrogen bond transfers from the phenol to the nitrogen of the base. The combination of ET to form the tyrosyl radical and PT from the phenol to the histidine comprises the PCET system. In a succeeding reaction, the tyrosyl radical formed can then be reduced in the S-state cycle that transfers a hydrogen atom from water bound to the manganese cluster, as displayed in Figure 1, Reaction 2. This scheme can be viewed as either consecutive reactions of ET/PT or PT/ET or as a concerted, hydrogen-atom transfer $Y_ZO^{\bullet}/Mn(H_2O)$ HAT $\xrightarrow{HAT}$ Y_ZOH/Mn^+ (OH^-). We suggested[41] that the $Y_Z^{\bullet}$ reduction occurs by a concerted process.

Figure 2 schematizes possible charge-transfer pathways where pathways a and b are consecutive and correspond, respectively, to ET followed by PT (ET/PT) and PT followed by ET (PT/ET), while the concerted pathway is c and denoted as ETPT. The electron/proton-transfer complex is denoted as DNHOA, and the charges on D, N, O, A, and H distinguish the different possible chemical species. In each charge-transfer event, ET, PT, and ETPT, the potential surface—one-dimensional for the electron (ET) or for the proton (PT) and two-dimensional for the electron and proton in ETPT—depends parametrically on the nuclear coordinates of the surrounding medium. The quantum tunneling takes place when a medium thermal fluctuation symmetrizes the one-dimensional surface for ET or for PT or symmetrizes the two-dimensional surface for ETPT.[6−8] Which quantum event is permitted (by symmetrization of the respective potential surfaces), in response to medium fluctuations, distinguishes the different charge-transfer mechanisms. Which pathway will dominate is an issue of competitive rates that will be determined by electronic structure effects of the reactants and products, as well as by the coupling of the electron's and proton's reactant and product state charge distributions to the surrounding medium that, in biological contexts, typically consists of proteins, cofactors, bound and free water, and various ions. If, for example, the solvation energetics dictates that the ET reaction in pathway a is strongly endoergic, then it is unlikely that this will be a competitive pathway. Even if the following

† This work is dedicated to the memory of Gerald T. Babcock; a superb scientist, colleague, and friend.

10.1021/jp012396m CCC: $22.00
Published on Web 01/18/2002

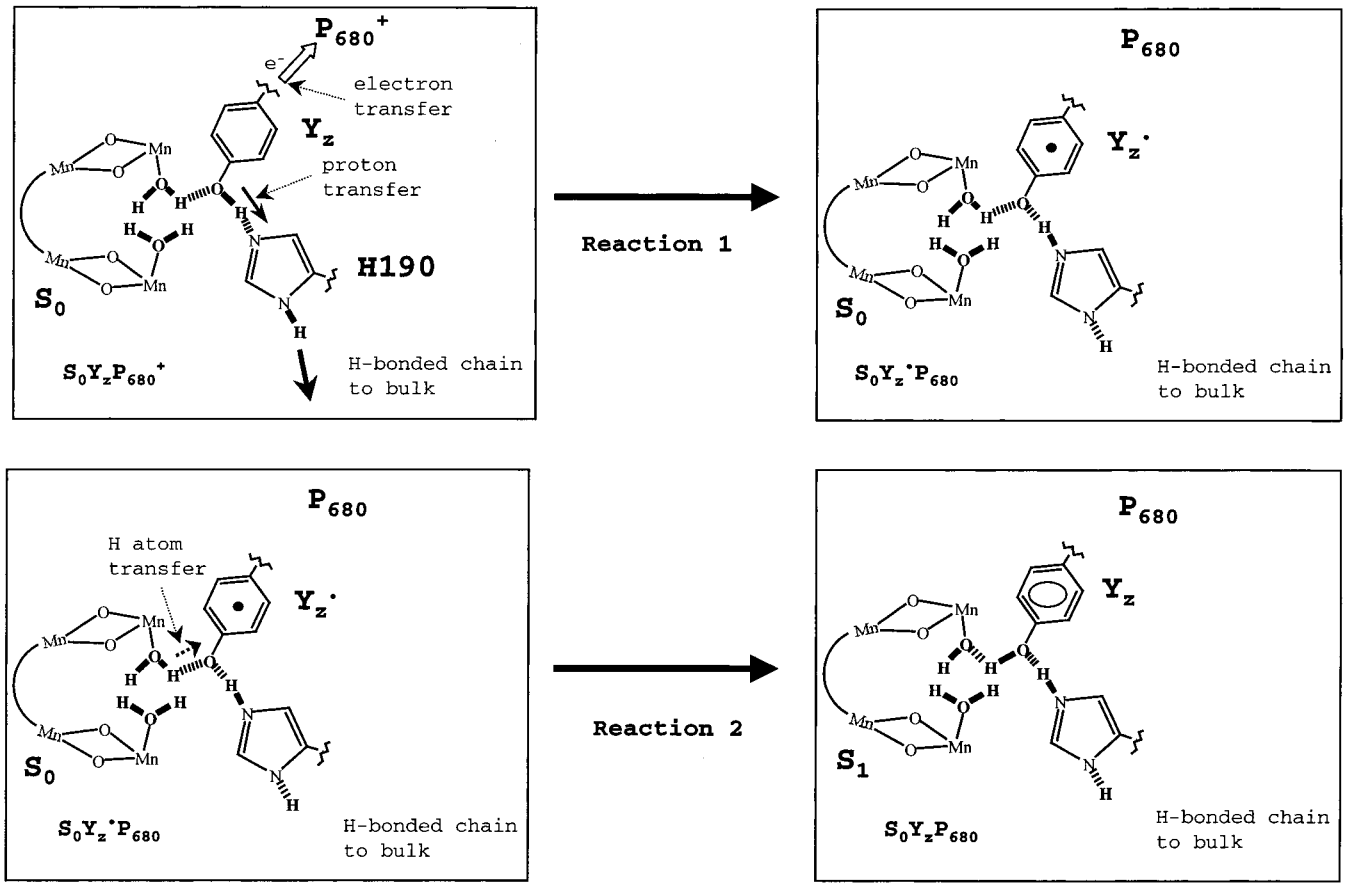

Figure 1. Hydrogen atom abstraction model for photosynthetic water oxidation. The catalytic center of PSII is postulated to be arranged as drawn. Substrate water binds terminally to the Manganese ions within hydrogen bonding distance (·····) of the Y_Z phenol group. Open arrows show the flow of electrons and solid arrows the flow of protons for the oxidation of Y_Z (Reaction 1). Oxidation of Y_Z is considered to be a proton-coupled electron-transfer reaction. The dotted arrow shows the H-atom transfer to $Y_Z^{\bullet}$, from the water bound to the $(Mn)_4$ cluster (Reaction 2). Reduction of $Y_Z^{\bullet}$ is considered to be a hydrogen atom transfer reaction.

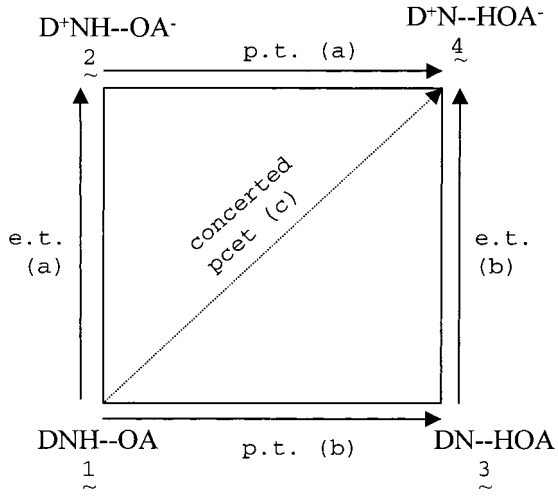

Figure 2. General scheme for PCET of a transfer complex DNHOA, with D (A) an electron donor (acceptor), and H hydrogen bonded between a nitrogen (N) and oxygen (O). The (---) line indicates a hydrogen bond. Pathways a and b are consecutive schemes—ET followed by PT and PT followed by ET, respectively. Pathway c is concerted ETPT. If, in pathway a, ET is highly endoergic, the PT step may be highly exoergic, but due to the rate limiting step principle, the overall rate will be small. The tunneling path for concerted ETPT is correspondingly longer than those for individual ET and PT steps, so the ETPT rate constant is limited by this effect.

PT reaction is fast, consecutive reaction schemes are limited by their slow step. On the other hand, the concerted transfer of an electron and proton may be more difficult than individual transfers, as these reactions occur by the intrinsically low-probability event of quantum mechanical tunneling, and transferring two quantum particles simultaneously can be difficult. When evaluating rate constants for ETPT we assumed that, because the proton wave functions are quite localized on a molecular scale, the interaction between their charge distributions and the solvent should not have a strong dependence on the proton's quantum state. In this regard, a recent theory of PCET has gone beyond this assumption and constructed a continuum-based theory that accounts for specific effects of solvation on the various proton states that are coupled in the transfer.[15]

In our previous work, we concentrated on the situation where the electron and proton have different sources within a reaction complex, as indicated in Figure 1, Reaction 1. The electron is perforce tunneling a long distance; consequently, the appropriate description is in terms of weak coupling between donor and acceptor (the nonadiabatic ET regime). For the proton, we assumed that its transfer could also be described by a weak coupling, nonadiabatic theory. The PCET theory we constructed, appropriate to both consecutive and concerted processes, made use of the assumed nonadiabatic behavior for electron and proton. In this work, we generalize our theory to the regime where the electron is considered as adiabatic and the proton can be nonadiabatic-to-adiabatic in its description. The generalization is carried out with a Landau−Zener-based[45−47] approach that provides an approximate way to span the nonadiabatic-

to-adiabatic regimes for curve-crossing problems. The motivation is the characterization of hydrogen-atom transfer. For HAT, the electron is transferring a relatively short distance (on the scale of a hydrogen-bond distance), as appropriate to Reaction 2 in Figure 1, and its transfer should be considered as an adiabatic process. Indeed, in this situation, distinguishing a particular electron loses meaning and one electronic potential energy surface for the proton that simultaneously characterizes the electronic redistribution should suffice. The importance of the degree of adiabaticity to theories of ET, PT, PCET, and atom transfer in general was noted early on[3,17,48] and plays a prominent role in the PT approaches of Borgis and Hynes[49] and Cukier and Zhu[50] and the PCET approach of Hammes-Schiffer and co-workers[13,14] and Georgievskii and Stuchebrukhov.[18]

An important experimental probe of reaction mechanism is the measurement of isotope effects.[51] In the typical biological reaction mechanism that consists of a sequence of steps, isolating the rate-limiting step can be arduous, and the presence or absence of isotope effects is used to come to conclusions as to which step is being probed. Furthermore, the relative rates of proton and deuteron reactions (kinetic isotope effect (KIE) measurements) are used to infer the nature of the transfer, i.e., a tunneling or overbarrier reaction.[52] The interpretation of KIEs relies on a model for the transfer process. If the transfer mechanism is through-barrier tunneling, the KIEs tend to be large, since, for a given potential energy surface, a proton can tunnel much more efficiently than a deuteron. We will demonstrate below that isotope effects are not necessarily large, even though the transfer proceeds by tunneling. The effect arises from the dominance of adiabatic proton transfer when the configurations of the heavy-atom framework that surround the transferring group correspond to smaller-than-equilibrium heavy-atom distances. Krishtalik[52] was the first to point out the key role that the heavy-atom distance plays in modulating the isotope effect. The rate-constant expression that we obtain is a certain average over the distribution of heavy-atom distances. Its value will be controlled by close heavy-atom distances, where the effect of the difference in proton-versus-deuteron tunneling is greatly reduced. This will lead to relatively small isotope effects, as has been found for a number of HAT reactions. The reduction of isotope effects by the proton/deuteron becoming adiabatic has also been noted by Hammes-Schiffer and co-workers[13,14] and Georgievskii and Stuchebrukhov.[18]

Experimentally determined activation energies in some HAT systems are relatively small; yet the rates themselves are rather low, indicating a small preexponential factor. For ET and PT and ETPT in the nonadiabatic electron and nonadiabatic proton regime, this is an expected result, since the electronic coupling matrix element and the corresponding proton matrix elements (proton Franck−Condon factors) are small. For the regime of interest here, where the electron is adiabatic and the proton is mainly adiabatic, a small activation energy would lead to fairly large rate constants. We obtain expressions that incorporate inner-sphere vibrational modes into the above-noted average over heavy-atom distances and find that small rate constants, low activation energies, and small isotope effects can be expected for hydrogen-atom transfer reactions.

In section II, we review PCET theory to set the stage for its generalization to apply to HAT, which is obtained in section III. Incorporation of the heavy-atom framework dynamics on the HAT rate-constant expression is carried out in section III. In section IV, we numerically analyze the rate expression for its implications regarding isotope effects. Section V adds the influence of inner-sphere vibrational motion on the HAT rate constant. Section VI contains our concluding remarks and experimental comparisons.

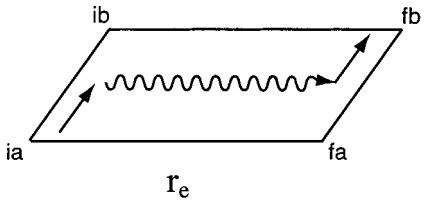

Figure 3. Zigzag tunneling path in a two-dimensional electron−proton tunneling space. The wavy line denotes the electron's tunneling when the proton rearranges to the proper configuration to symmetrize the electron potential energy surface. The straight arrows denote the proton's motion for the initial *i* and final *f* electron states.

II. Proton-Coupled Electron Transfer

If the consecutive reaction pathways a and b, indicated in Figure 2, dominate the kinetics, then the overall rate constant k has the form of a rate-limiting law:

$$k^{-1} = k_{et}^{-1} + k_{\mathrm{pt}}^{-1} \tag{2.1}$$

where k_{et} and k_{pt} are, respectively, electron- and proton-transfer rate constants.[8] If these rate constants can be formulated according to the Marcus-Levich[2,48,53,54] picture of charge-transfer reactions, then

$$k_{ct} = \frac{V_{ct}^{\ 2}}{\hbar}\sqrt{\frac{\pi}{\lambda_s k_B T}}\, \mathrm{e}^{-(\lambda_s+\Delta G^0)^2/4\lambda_s k_B T} \qquad (c = e, p) \tag{2.2}$$

where the characteristic parameters that come from the coupling of the reactant and product charge distributions to the surrounding medium are the solvent reorganization (λ_s) and reaction-free (ΔG^0) energies. When the reactant and product states are weakly coupled (nonadiabatic reactions), V_{ct} is the electronic (protonic) matrix element V_{et} (V_{pt}). For stronger coupling (adiabatic reactions), the prefactor $V_{ct}^2/\hbar\sqrt{\lambda_s k_B T}$ is replaced by $\omega_s/2\pi$, where ω_s characterizes the rate of solvent orientational polarization fluctuations.

Turning to pathway c, the concerted mechanism, a view of the process can be formulated in a two-dimensional tunneling space,[6] whereby electron and proton are both treated as quantum objects that must both tunnel through a two-dimensional profile that is parametric on the nuclear coordinates of the surrounding medium. This treats the electron and proton on an equal footing. The shape of the two-dimensional potential energy surface that is parametric on the solvent coordinate couples the electron and proton via their respective charge distributions. The solvent configurations that permit the concerted transfer of the electron and proton by symmetrizing the two-dimensional surface reflect the coupling between electron and proton. However, the mass disparity between the two suggests a simplification of this two-dimensional tunneling problem when the solvent has fluctuated to an appropriate configuration. The tunnel path can be restricted by letting the proton displace adiabatically along its coordinate until it reaches a position that permits the electron to tunnel (one-dimensionally) along its coordinate.[6] Then the proton, with the electron in its final state, relaxes to its final state. This zigzag tunnel path is illustrated in Figure 3, where *i* and *f* denote the initial and final electron states and *a* and *b* the initial and final proton states. Use of this zigzag path then leads to the following rate expression for ETPT:

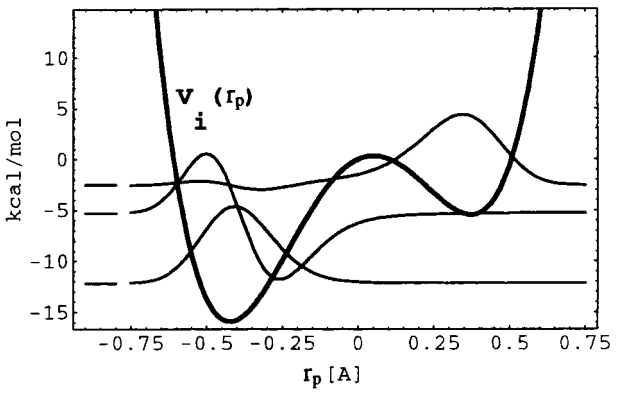

Figure 4. An initial electron state that supports both ET and ETPT reaction channels. The energies of the proton-localized levels are shown along with their corresponding wave functions. The pattern for the final electron state is obtained by inversion through the origin. In the initial electron state, the lowest proton (left-localized) proton state has good Franck−Condon overlap with the third proton state of the final electron state surface and can therefore permit a large ET rate constant.

$$k_{etpt} = \frac{V_{el}^{\,2}}{\hbar^2}\sqrt{\pi\hbar^2/\lambda_s k_B T}\sum_{n_i}\rho_{n_i}^{i}\sum_{n_f}|\langle\chi_{n_f}^{f}|\chi_{n_i}^{i}\rangle|^2 e^{-(\lambda_s+\Delta G^0+\epsilon_{nf}^{f}-\epsilon_{ni}^{i})^2/4\lambda_s k_B T} \quad (2.3)$$

This expression can also be obtained by a "double adiabatic" procedure,[6] as discussed by Ulstrup,[48] which relies on a separation of time scales with the electron faster than the proton and the proton faster than the solvent. The new ingredients are Franck−Condon factors of the initial (final) state proton vibronic wave functions $\chi_{n_i}^{i}$ ($\chi_{n_f}^{f}$). The initial states are thermally weighted over the equilibrium proton distribution in its initial state, $\rho_{n_i}^{i}$. The "effective" activation energy appearing in the exponent of eq 2.3 involves the energetic difference of the proton eigenstates, $\epsilon_{n_f}^{f} - \epsilon_{n_i}^{i}$, and arises from the requirement of overall energy conservation between the initial and final electron−proton states. The tunneling of the proton is manifested in the Franck−Condon factors in eq 2.3. Thus, concerted PCET is limited by a "FC drag" that is a reflection of the two-dimensional tunneling requirement.

For k_{etpt}, in addition to the quantities that arise for ET and PT, a model for the proton potential surfaces when the electron is in its initial and final state is required. Typically, these are double-well potentials that may support proton localized states on either side of the flanking heavy atoms. Then, FC factors can be obtained by evaluating the overlaps of the $\chi_{n_i}^{i}$ and $\chi_{n_f}^{f}$ corresponding to states of energy $\epsilon_{n_i}^{i}$ and $\epsilon_{n_f}^{f}$ for the proton when the electron is in its initial and final states. A representative potential surface, along with wave functions for the bound levels, is shown in Figure 4. Note that there a just a few bound levels in such typical proton potential surfaces.

III. Hydrogen-Atom Transfer

We now consider reactions where the electron and proton form a hydrogen-atom transfer (HAT) system. While we have indicated in the Introduction that a HAT description is appropriate for an electron and proton transferring in spatial proximity, a more precise distinction can now be made. Since the electron is tunneling a distance comparable to that of the proton, the electronic matrix element V_{el} that couples the electron in its initial and final states will typically become sufficiently large that a diabatic, localized-state representation is no longer an appropriate basis. Indeed, for strong electronic coupling, distinguishing a transfer electron is no longer a useful concept, and one should change to an adiabatic viewpoint of a smooth change in electronic structure of the molecule.

From the perspective of the formalism of section II, the way to proceed is by converting to the adiabatic surfaces formed from the two diabatic surfaces, $\epsilon_i(r_p)$ and $\epsilon_f(r_p)$, and the electronic matrix element that couples them.[47,55] Adiabatic (electronic) surfaces are illustrated in Figure 5, where they are sufficiently split in the interaction region that only $\epsilon_+(r_p)$ is thermally accessible. The "matrix element" connecting the proton−electron (transferring hydrogen) initial and final states is the difference $\Delta\epsilon$ between the two lowest energy levels in the $\epsilon_+(r_p)$ surface. The $\Delta\epsilon$ in Figure 6 was obtained by solving the Schrödinger equation by expansion in a sufficiently large harmonic oscillator basis to ensure convergence to the correct wave functions and energies. The potential surface used was a quartic fit to a Lippincott Schroeder form.[56−58] The Lippincott Schroeder surface is often used to parametrize hydrogen-bond potential energy surfaces for proton (hydrogen-atom) transfers, when it is important to characterize the dependence of the potential on the heavy-atom flanking atom separation that we denote generically as R_{AB}. For the parameters appropriate to Figure 6, $R_{AB} = 2.6$ Å, slightly less than the equilibrium distance of 2.7 Å.

The potential surface drawn in Figure 5 is symmetric; there are also asymmetric surfaces where, in a localized wave function

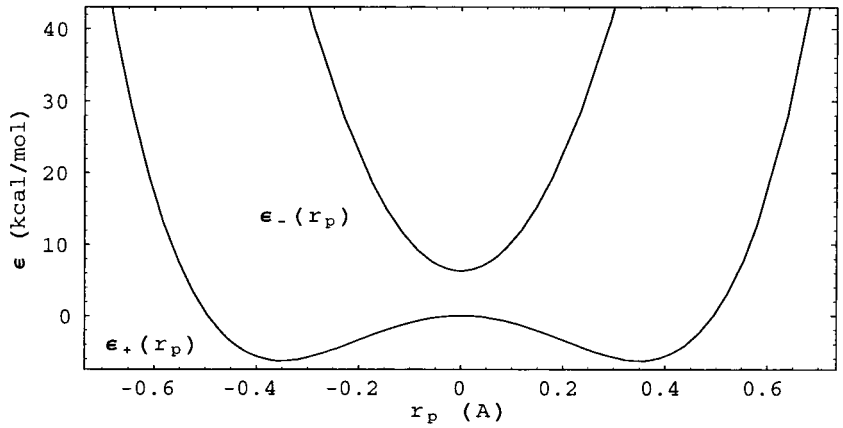

Figure 5. Schematic adiabatic potential surfaces, ϵ_+ and ϵ_-, formed from diabatic surfaces that are mixed by a coupling term in the region where the diabats are close in energy. If the energetic difference between the adiabatic surfaces in the mixing region is large compared with kT, then only the lower (electronically) adiabatic surface is required.

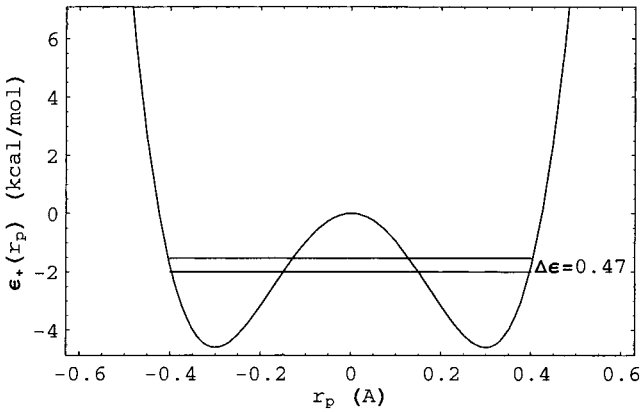

Figure 6. Splitting $\Delta\epsilon$ between the two lowest eigenstates of the ϵ_+ surface. The potential surface used was a quartic fit to a Lippincott Schroeder form for an amine−carboxylate hydrogen bonded system, with a heavy atom distance $R_{AB} = 2.6$ Å, slightly less than the equilibrium distance of 2.7 Å.

representation, the energy of the proton (hydrogen) on the left and right sides would be equal. (Recall that these potential surfaces are parametric on the nuclear coordinates of the surrounding medium.) For various degrees of solvation, it is possible to get such degenerate states in the local basis. These localized states with quantum numbers n_i and n_f will mix to provide delocalized states whose separations $\Delta\epsilon_{n_i n_f}(R_{AB})$ would also provide a transfer mechanism. For reactions where the electronic structure upon proton transfer greatly shifts the proton stability, the ground-state-to-ground-state transition should be dominant, so we will restrict the development to this $\Delta\epsilon \equiv \Delta\epsilon_{00}(R_{AB})$ coupling.

The role of R_{AB} dynamics is critical to a proper formulation of HAT.[52] Schematically,

$$\begin{array}{l} \mathrm{A-H\cdots\cdots B} \longleftrightarrow \mathrm{A\cdots\cdots H-B} \\ \quad\; |\leftarrow \mathrm{R_{AB}} \rightarrow| \end{array}$$

The changing R_{AB} will strongly modulate $\Delta\epsilon$.[59,60] When the separation R_{AB} decreases, the barrier in the $\epsilon_+(r_p)$ proton surface decreases and the corresponding $\Delta\epsilon$ increase—in principle, spanning behavior from the nonadiabatic to adiabatic regimes for the hydrogen atom. Note that $\Delta\epsilon$ can be calculated parametrically on the R_{AB} distance, since characteristic R_{AB} vibrational frequencies are low ($\sim$200 cm^{-1}) relative to hydrogen-atom frequencies ($\sim$2000 cm^{-1}).[60]

An appropriate approach to span these regimes is to use Landau−Zener (LZ) theory.[45−47] In previous work,[50] we have used a LZ approach for pure proton-transfer reactions. Here, we adapt this approach to HAT. The LZ theory is formulated in terms of diabatic coupling elements $V_{n_i n_f}(R_{AB})$ that are related to the adiabatic surface energy separations via $\Delta\epsilon_{n_i n_f}(R_{AB}) = 2V_{n_i n_f}(R_{AB})$. To incorporate the effect of the R_{AB} dynamics on HAT, we first indicate how it enters a nonadiabatic PT expression. Then, we will show how a formally similar expression can be generated for HAT. A number of approaches have been proposed to include the R_{AB} effects on pure PT;[49,52,61−67] we summarize our method, as it provides a direct route to incorporate the Landau−Zener-based generalization to span nonadiabatic to adiabatic regimes. First, note that, for PT, the expression in eq 2.3 simplifies to just one term (with no V_{el}^2 factor), where the one FC factor that appears refers to the particular proton-transfer states being connected, for example, the $n_i = n_f = 0$ states with $V_{n_i=0 n_f=0}(R_{AB}) \equiv V_{00}(R_{AB})$. The FC factor can be expressed in terms of the protonic matrix element $|\langle\chi^i_{n_i=0}|\chi^f_{n_f=0}\rangle| = V_{00}(R_{AB})/\hbar\omega$, using semiclassical arguments.[47,54] (Indeed, the FC factors between any pair of tunnel states n_i and n_f can be expressed in terms of a tunnel-splitting, $V_{n_i n_f}$, for those states divided by the well energy $\hbar\omega$; $\langle\chi^i_{n_i}|\chi^f_{n_f}\rangle = V_{n_i n_f}/\hbar\omega$.) A golden-rule derivation in the perturbation $V_{00}(R_{AB})$ will, as shown in Appendix A (cf. eq A.6), lead to the rate-constant expression

$$k_{pt} = \sqrt{\pi/\hbar^2\lambda_s k_B T}\sum_{\mu_i}\rho^i_{\mu_i}\sum_{\mu_f}|V_{00}^{\mu_f\mu_i}|^2 \mathrm{e}^{-(\lambda_s+\Delta G^0+E_{\mu_f}{}^f-E_{\mu i}{}^i)^2/4\lambda_s k_B T} \tag{3.1}$$

where the origin of the sums over the matrix elements

$$V_{00}^{\mu_f\mu_i} = \langle\varphi^i_{\mu_i}(R_{AB})|V_{00}(R_{AB})|\varphi^f_{\mu_f}(R_{AB})\rangle \tag{3.2}$$

is the R_{AB} dependence of $V_{00}(R_{AB})$, a non-Condon effect. The wave functions $\varphi^i_{\mu_i}(R_{AB})(\varphi^f_{\mu_f}(R_{AB}))$ are those characterizing the heavy-atom framework motion when the proton is in its initial (final) state.

A rate constant that spans the nonadiabatic to adiabatic regimes can be constructed from the LZ parameters:

$$\bar{v}_{00}^{\mu_i\mu_f} \equiv (v_{00}^{\mu_i\mu_f}/v_T) = \frac{2\pi(V_{00}^{\mu_i\mu_f})^2}{\hbar\omega_s\sqrt{2\lambda_s k_B T}} \tag{3.3}$$

where $v_T = \sqrt{k_B T/m_s}$ is the thermal velocity. The LZ parameter controls the efficiency of a quantum transition—when it is small the transition probability is small; when it is large, the transition probability approaches one. The rate constant may be approximated in the form[50]

$$k_{pt} = \frac{\omega_s}{2\pi}\sum_{\mu_i}\rho^i_{\mu_i}\sum_{\mu_f}A_{00}^{\mu_i\mu_f}\mathrm{e}^{-(\lambda_s+\Delta G^0+E_{\mu_f}{}^f-E_{\mu i}{}^i)^2/(4\lambda_s k_B T)} \tag{3.4}$$

where

$$A(\bar{v}_{00}^{\mu_i\mu_f}) = [1-\mathrm{e}^{-\bar{v}_{00}{}^{\mu i\mu f}}][1-\mathrm{e}^{-\bar{v}_{00}{}^{\mu i\mu f}}/2]^{-1}\left[(1-\mathrm{e}^{-2\bar{v}_{00}{}^{\mu i\mu f}}) + \frac{\sqrt{\pi}}{2}\mathrm{e}^{-2\bar{v}_{00}{}^{\mu i\mu f}}\right] \tag{3.5}$$

The form of eqs 3.2−3.5 is an approximation to what is an average over all nuclear velocities. We previously showed that the above expression for $A_{00}^{\mu_i\mu_f}$, given in terms of the thermal velocity, is an excellent approximation to the velocity average. The parameters in eqs 3.1−3.5 are the solvent reorganization energy, $\lambda_s = m_s\omega_s^2 d^2/2$, defined by an effective mass for the orientational polarization of the solvent and the displacement, d, between the equilibrium points of the solvent surfaces upon the HAT. The characteristic solvent frequency is $\omega_s = \sqrt{\langle(\delta v_s)^2\rangle/\langle(\delta x_s)^2\rangle}$, with δx_s and δv_s, the deviations from equilibrium of the solvent polarization coordinate and its corresponding velocity, respectively.[68] Equations 3.4 and 3.5 define a quantity, $A_{00}^{\mu_i\mu_f}$, which is a "pure" (without activation energy) Landau−Zener transition probability.

The k_{pt} expression interpolates between the (protonic) nonadiabatic (NA) limit given in eq 3.1 and the (protonic) adiabatic (A) limit:

$$k_{pt} = \frac{\omega_s}{2\pi}\sum_{\mu_i}\rho^i_{\mu_i}\sum_{\mu_f} e^{-(\lambda_i+\Delta G^0+E_{\mu f}{}^f-E_{\mu i}{}^i)^2/4\lambda_s k_B T} \quad (3.6)$$

Limiting forms similar to these have been obtained before.[3,48]

For ETPT/HAT, there are manifolds of proton states n_i and n_f before and after charge transfer, as displayed in eq 2.3 for ETPT. The proton splittings between any pair of protonic states $V_{n_i n_f}(R_{AB}) = \langle\chi^i_{n_i}|\chi^f_{n_f}\rangle\hbar\omega$ will give the Franck−Condon-based factors

$$\Omega^{\mu_i\mu_f}_{n_i n_f} \equiv \langle\varphi^i_{\mu_i}(R_{AB})|\langle\chi^i_{n_i}|\chi^f_{n_f}\rangle(R_{AB})|\varphi^f_{\mu_f}(R_{AB})\rangle_{R_{AB}} \quad (3.7)$$

Thus, if R_{AB} effects are to be included in a general fashion, then each term in the double sums over protonic states n_i and n_f in eq 2.3 will, in turn, become double sums over μ_i and μ_f of the matrix elements of the FC factors between wave functions of the possible before-and-after-HAT states of the R_{AB} motion, the $|\Omega^{\mu_i\mu_f}_{n_i n_f}|^2$.

Let us now restrict the proton states involved in HAT to the $n_i = n_f = 0$ states. In this case, the quadruple sum reduces to a double sum. Then, as shown in Appendix A (cf., eq A.7), we obtain, again with the assumption of a classical solvent

$$k_{HAT} = \frac{V_{el}{}^2}{\hbar}\sqrt{\pi/\lambda_s k_B T}\sum_{\mu_i}\rho^i_{\mu_i}\sum_{\mu_f}|\Omega^{\mu_i\mu_f}_{00}|^2 e^{-(\lambda_s+\Delta G^0+E_{\mu f}{}^f-E_{\mu i}{}^i)^2/4\lambda_s k_B T} \quad (3.8)$$

A comparison of eqs 3.8 and 3.1 show that they have the same structure. Thus, we may construct a LZ theory for k_{HAT}, using the same methods as we used previously for k_{PT}.

For the purposes of HAT, there are physically motivated approximations that will provide a much simpler and transparent expression than that required for PT. Namely, we shall assume that the reorganization energy associated with the R_{AB} motion is minimal. This feature follows from the similar hydrogen bond strengths of H···B and A···H. Therefore, the potential surfaces before and after HAT should be quite similar. In addition, the displacement of the before-and-after-HAT equilibrium R_{AB} distances should be minimal, and the characteristic frequency of the motion is low. These conditions lead to small reorganization energies. We have indeed found these features in simulations of phenol-amine potential energy surfaces.[50] With these assumptions, an easily interpretable expression for the HAT rate constant, including the effects from the R_{AB} modulation, can be obtained, as shown in Appendix B. The HAT rate constant can be written in the form

$$k_L = \int dR_{AB}\, P(R_{AB}) k^{LZ}_{L,00}(R_{AB}) \qquad (L = H, D) \quad (3.9)$$

where $P(R_{AB})$ is the thermally averaged probability of observing the heavy-atom distance R_{AB}, and we use the "L" subscript to refer to atom transfer of hydrogen $L = H$ or deuterium $L = D$.

The Landau−Zener parameter that appears in $k^{LZ}_{L,00}(R_{AB})$ is defined as

$$\bar{v}_{00}(R_{AB}) \equiv v_{00}(R_{AB})/v_T = 2\pi V_{00}{}^2(R_{AB})/\hbar\omega_s\sqrt{2\lambda_s k_B T} \quad (3.10)$$

and replaces the $\bar{v}^{\mu_i\mu_f}_{00}$ in eq 3.5 to give $A(\bar{v}_{00}(R_{AB})) \equiv A^{LZ}_{00}(R_{AB})$. While the expression in eq 3.9 is appealing in its physical formulation as an average of an R_{AB} dependent LZ rate constant over the equilibrium distribution $P(R_{AB})$ of R_{AB} distances, it does depend on the approximations noted above. The notation in eq 3.9 emphasizes that $k^{LZ}_{L,00}(R_{AB})$ depends on the isotope while $P(R_{AB})$ does not.

IV. Analysis of the HAT Expression

The Landau−Zener R_{AB} averaged rate constant in eq 3.9 depends critically on the distance dependence of $\Delta\epsilon(R_{AB}) = 2V_{00}(R_{AB})$. In previous work,[50] we used a Lippincott−Schroeder[56] potential energy surface and solvated it with the electronic polarization component of a polar liquid (dichloromethane) to obtain a proton−electronically solvated surface $V_{pels}(r_p,R_{AB})$. The requirement for solvation by electronic polarization of the gas phase Lippincott−Schroeder surface recognizes that, since the electronic polarization is fast relative to the hydrogen atom dynamics, the true surface is actually a potential of mean force.[50] It is the same solvation that is used in the Marcus theory for electron transfer and is responsible there for the appearance of the optical (high-frequency) dielectric constant in the solvent reorganization energy.[54] A fit of $V_{00}(R_{AB}) = \Delta\epsilon_{00}(R_{AB})/2$ for varying R_{AB} distances gave

$$V_{00}(R_{AB}) = V^0_{00} e^{-\alpha(R_{AB}-R_{AB}{}^{eq})} \quad (4.1)$$

with $R^{eq}_{AB} = 2.7$ Å, $V^0_{00} = 0.045$ kcal/mol and $\alpha_H = 35$ Å^{-1}. For deuterium, the corresponding parameters are $V^0_{00} = 0.005$ kcal/mol and $\alpha_D = 1.4*35$ Å^{-1}. The exponential dependence on R_{AB} is expected from the feature that the size of $V_{00}(R_{AB})$ is set by the overlap of the exponential tails of the wave function when it is thought of as localized in its initial or final side. As $V_{00}(R_{AB})$ increases to where it is substantial relative to the well depth of the potential surface, this exponential dependence goes over to a linear dependence on R_{AB}.[49] The error made by assuming an exponential form will be negated by the feature that the LZ factor saturates to unity and that the $P(R_{AB})$ factor becomes very small in this small R_{AB} regime. For a given value, the deuterium splitting is much smaller than the splitting for protium, and the deuterium decay is faster than the decay for protium, as expected for the mass ratio of the isotopes. It is interesting that the R_{AB} dependence of $V_{00}(R_{AB})$, in the exponential decay regime, does scale with $\sqrt{m_D/m_H}$, as would be dictated by simple potential energy surface models and a WKB approximation to the splitting.[55]

The other quantities required for evaluating the LZ parameter are a solvent reorganization energy that is set to $\lambda_s = 2000$ cm^{-1}, as typical of a HAT process where minimal charge is moved, and $\omega_s = 10$ ps^{-1} that we[50] and others[68] have found, based on molecular-dynamics simulations of polar solvents, for the solvent relaxation frequency. Figure 7 displays the Landau−Zener probability $A^{LZ}_{00}(R_{AB})$ defined in eqs 3.5 and 3.10 for hydrogen (H) and deuterium (D). As R_{AB} becomes sufficiently small, where the barrier in the potential surface is much reduced and the splitting $V_{00}(R_{AB})$ becomes relatively large, $A^{LZ}_{00}(R_{AB})$ saturates to unity. The transition region is shifted inward for D versus H.

The thermal probability of observing different R_{AB} distances depends on whether one is dealing with an intramolecular-bonding situation or a bimolecular-repulsive potential for this coordinate. For a bond potential, the thermal distribution function is

$$P_{bond}(R_{AB}) = (1/\sqrt{2\pi\langle(\delta R_{AB})^2\rangle})e^{-(\delta R_{AB})^2/2\langle(\delta R_{AB})^2\rangle} \quad (4.2a)$$

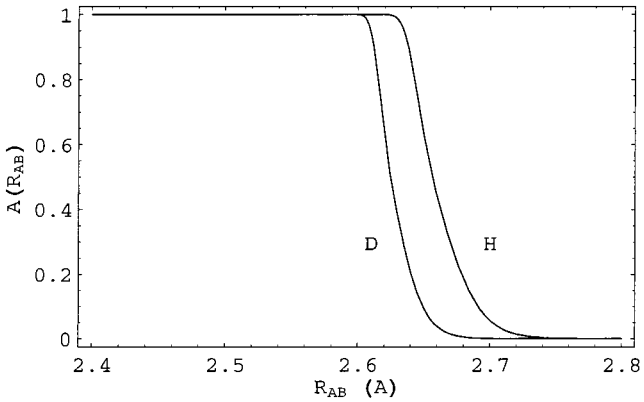

Figure 7. Landau−Zener probabilities $A_{00}^{LZ}(R_{AB}) \equiv A(R_{AB})$ for H and D, defined in eqs 3.5 and 3.10, and for $V_{00}(R_{AB})$ as given by eq 4.1 and other parameters specified there.

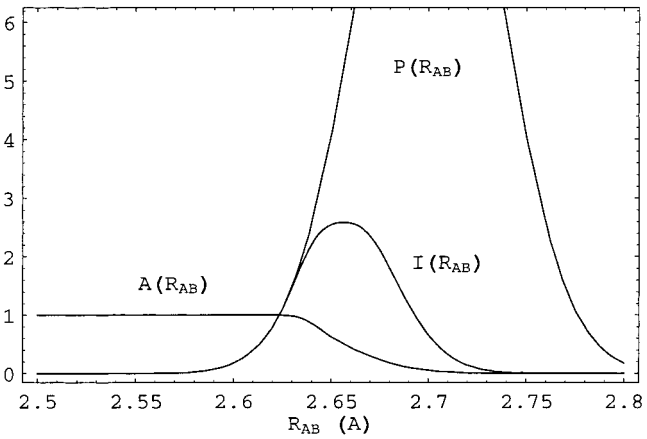

Figure 8. $I_H(R_{AB})$, the product of the Landau−Zener probability $A_{00}^{LZ}(R_{AB})$ for hydrogen, and the bond thermal probability $P_{bond}(R_{AB})$ defined in eq 4.2. The behavior of the product is to shift the peak in relative to $P_{bond}(R_{AB})$, thus emphasizing the smaller-than-equilibrium values of R_{AB}.

where

$$\langle(\delta R_{AB})^2\rangle = (\hbar/\mu\omega)\coth(\beta\hbar\omega/2) \qquad (\delta R_{AB} = R_{AB} - R_{AB}^{eq}) \tag{4.2b}$$

The bond probability becomes more peaked about the equilibrium separation, as the reduced mass μ or the frequency ω characterizing the heavy-atom coordinate increases.

The isotope effect can be explored most directly by plotting $I_L(R_{AB})$, the product of $P_{bond}(R_{AB})$ and $A_{00}^{LZ}(R_{AB})$. Note that $A_{00}^{LZ}(R_{AB})$ does not depend on the activation energy; it is the pure LZ factor (cf. eqs 3.4, 3.5, and 3.10). In Figure 8, we display this product (for the H case) denoted as $I_H(R_{AB})$, which shows a peak that is shifted in from the maximum of $P_{bond}(R_{AB})$. The plot of $I(R_{AB})$ for H and D in Figure 9 demonstrates the general feature that the integrand is smaller for D versus H, indicating the scale of the isotope effect.

Table 1 lists the integrated results

$$I_L = \int \mathrm{d}R_{AB}\, P(R_{AB}) A_{00}^{LZ}(R_{AB}) \equiv \int \mathrm{d}R_{AB}\, I_L(R_{AB}) \tag{4.3}$$

for H and D and the ratio to be expected for the rate constants. (The values for the I_L are, of course, not rate constants.) When the integral's value is dominated by R_{AB} distances where $k_{L,00}^{LZ}(R_{AB})$ is in the adiabatic limit, $A_{00}^{LZ}(R_{AB}) \rightarrow 1$ and $I_L \rightarrow 1$. In regime when the integral's value is dominated by R_{AB} distances where $k_{L,00}^{LZ}(R_{AB})$ is in the nonadiabatic limit,

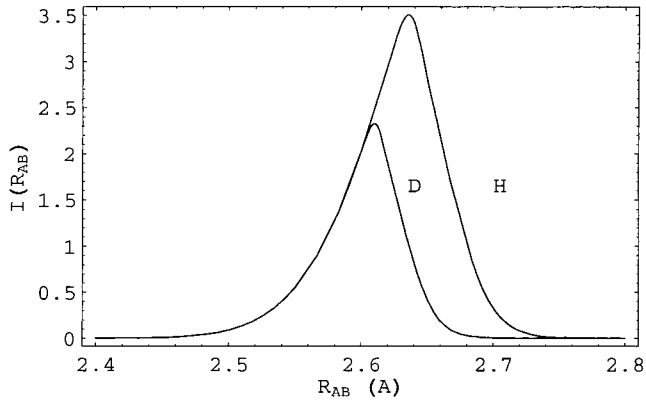

Figure 9. $I_L(R_{AB})$ (L=H, D), defined in eq 4.3, using the thermal bond probability (cf. eq 4.2) showing that the D-curve is smaller than that for H, reflecting the smaller Landau−Zener factor $A_{00}^{LZ}(R_{AB})$ for D vs H for a given R_{AB} value. This behavior arises from the reduced tunneling of D relative to H. See eq 4.1 and following for parameter values.

TABLE 1: Kinetic Isotope Effect for a Bond Potential

ω (cm^{-1})[a]	μ (amu)[b]	I_H	I_D	k_H/k_D
150	30	0.3001	0.1636	1.83
150	60	0.2947	0.1552	1.90
220	30	0.2316	0.0810	2.85
220	60	0.1684	0.0307	5.49

[a] Heavy-atom framework vibrational frequency for equilibrium distance $R_{AB}^{eq} = 2.7$ Å. [b] Heavy-atom framework reduced mass.

$A_{00}^{LZ}(R_{AB}) \sim \bar{v}(R_{AB}^{eq}) \sim V_{00}^2(R_{AB}^{eq}) \equiv (V_{00}^0)^2$. Then, $I \sim (V_{00}^0)^2$ and is arbitrarily small. As the "quantum length" $l = \sqrt{\hbar/\mu\omega}$ decreases, the ratio k_H/k_D increases. For the values used here that are representative of typical nitrogen−oxygen heavy-atom hydrogen bonds, the isotope effect is clearly quite modest, in comparison with what would be predicted from using the equilibrium distance R_{AB}^{eq} and constructing a theory based on a nonadiabatic proton. Namely, note from eq 2.2 for proton transfer that k_H/k_D is proportional to the ratio of the squares of the respective V_{00} factors that would produce $k_H/k_D \approx 80$, based on the V_{00} values given after eq 4.1, for the R_{AB}^{eq} distance.

For an unbound R_{AB} potential surface, the equilibrium distribution function is related to the potential surface as

$$P_{rep}(R_{AB}) = \mathrm{e}^{-V_{pels}(R_{AB})/kT} \tag{4.4}$$

We model the unbound potential as the repulsive branch of a Morse potential

$$V_{pels}(R_{AB}) = D_e(\mathrm{e}^{-\kappa(R_{AB}-R_{AB}^{eq})} - 1)^2 \qquad R_{AB} \le R_{AB}^{eq} \tag{4.5}$$

and zero otherwise, since it is a good representation of the electronic repulsion in the context of hydrogen abstraction by radicals.[69] The parameters $D_e = 6.1$ kcal/mol and $\kappa = 5.11$ Å^{-1} are used as representative values. For $R_{AB}^{eq} = 2.650$ Å, the product of $A_{00}^{LZ}(R_{AB})$ and $P_{rep}(R_{AB})$, again denoted as $I(R_{AB})$, is displayed in Figure 10. The shape is quite similar to the analogous plot in Figure 9 for the bond potential.

Table 2 lists values of the integral of $I(R_{AB})$ (cf. eq 4.3) for varying values of R_{AB}^{eq}. A smaller value of R_{AB}^{eq} leads to a smaller k_H/k_D ratio, since the difference between the LZ probabilities, $A_{00}^{LZ}(R_{AB})$ for H and D, is minimized in this case. There is a greater range of isotope effect relative to the bond potential case; for a repulsive potential, there is more freedom

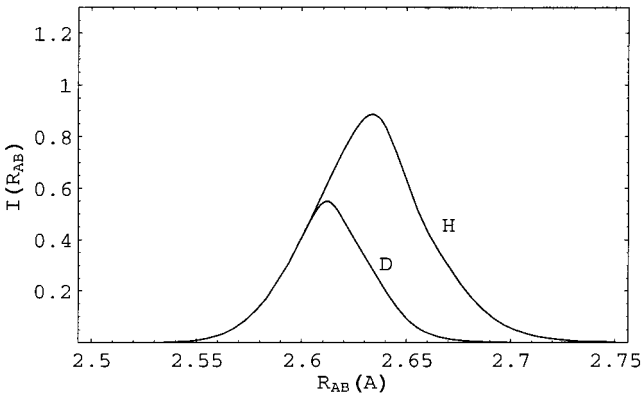

Figure 10. $I_L(R_{AB})$ (L=H, D), defined in eq 4.3, using the repulsive potential model defined in eqs 4.4 and 4.5. The shapes of the curves are similar to those for the thermal bond model displayed in Figure 9. See eq 4.5 and following for parameter values.

TABLE 2: Kinetic Isotope Effect for a Repulsive Potential

R_{AB}^{eq} (Å)[a]	I_H	I_D	k_H/k_D
2.600	0.0960	0.0632	1.520
2.625	0.0740	0.0411	1.795
2.650	0.0493	0.0193	2.551
2.675	0.0266	0.0060	4.469
2.700	0.0108	0.0011	9.450
2.725	0.0033	0.0001	22.848

[a] Equilibrium distance for Morse (repulsive branch) potential defined in eqs 4.4 and 4.5, with $D_e = 6.1$ kcal/mol and $\kappa = 5.11$ Å^{-1}.

in the repulsive potential surface. Note the sensitivity of k_H/k_D to small changes in the value of R_{AB}^{eq}.

V. Inclusion of Inner-Sphere Modes

Some reactions that can be considered to be hydrogen-atom transfers have rather small rate constants and, at the same time, have fairly small measured activation energies. At first glance, this seems puzzling, from the perspective presented here. If HAT is considered to be an electronically adiabatic process and to be in a regime where the isotope effects are modest so that the average over R_{AB} is dominated by the adiabatic limit for the proton, then calculated rate constants should tend to be large. A possible resolution of this seeming contradiction is to note that HAT processes can involve rather large inner-sphere reorganization energies. That is, there may be a substantial rearrangement of the nuclear framework upon HAT. For example, in Figure 1, Reaction 2, for the reduction of $Y_Z^{\bullet}$, there are substantial changes in the Mn−O equilibrium bond lengths upon HAT.[70] If these modes have characteristic frequencies large compared to thermal energy, then they will provide a pre-exponential factor that is rather small. Such quantum modes do not contribute to the activation energy.

To explore this issue, we augment the PCET/HAT theory to include inner-sphere vibrations.[71,72] Within the same set of approximations that leads to eq 3.9, regarding the role of the R_{AB} dynamics, it is straightforward to obtain the result

$$k_L = \frac{\omega_s}{2\pi}\int \mathrm{d}R_{AB}\, P(R_{AB}) A_{L,00}^{LZ}(R_{AB}) \otimes \Delta\sqrt{2/\pi}\int_0^\infty \mathrm{d}t\, \mathrm{e}^{-(\Delta t)^2/2} \cos[(\Delta G^0 + \lambda_s)t + \sum_{i=0} S_i \sin(\Omega_i t)] \exp[\sum_{i=0} S_i \coth(\hbar\Omega_i/kT)(\cos(\Omega_i t) - 1)] \quad (5.1)$$

where $S_i = E_{r_i}/\hbar\Omega_i$ is the reorganization energy, E_{r_i}, of the ith inner-sphere mode in units of the mode energy, $\hbar\Omega_i$, ΔG^0 is the standard reaction free energy introduced in eq 2.2, and $\Delta^2 = 2\lambda_s kT/\hbar^2$ is defined for notational convenience. If the reorganization of the inner-sphere modes is negligible (all the S_i are essentially zero), then the time integral in eq (5.1) yields the activation energy factor displayed in eq 3.4. To the extent that there is inner-sphere reorganization of the high-frequency modes, the new factors in eq 5.1 will serve to reduce the preexponential factor of k_L.

Table 3 tabulates the evaluation of eq 5.1 for a number of combinations of ΔG^0 and λ_s values. A standard value of $I_L = \int \mathrm{d}R_{AB}\, I_L(R_{AB}) = 0.01$ was used to construct Table 3. The values are chosen to be essentially activationless, in the sense that $(\Delta G^0 + \lambda_s)^2/4\lambda_s \approx 0$. Without inner-sphere contributions, the activationless rate would be $I_L \times \omega_S/2\pi \sim 1.6 \times 10^{10}$ s^{-1}. Many atom-transfer reactions have low but nonnegligible activation energies (1−8 kcal/mol). The rates obtained, when the activation energy is small but nonnegligible, will be correspondingly reduced relative to those listed in Table 3.

VI. Concluding Remarks and Experimental Comparisons

In this work, we have shown how a hydrogen-atom transfer reaction can be viewed as a particular limit of a concerted proton-coupled electron-transfer reaction. The small mass of the electron relative to that of the proton, combined with the spatial correlation between the electron and proton initial and final states, implies that the electron is strongly coupled between its initial and final states. Therefore, its transfer should be adiabatic. For the proton, dependent on the heavy-atom framework distance and parameters related to the solvent, its transfer can span the nonadiabatic to adiabatic regimes.

On the basis of these ideas, an approximate expression for HAT that is an average over the heavy-atom separation R_{AB} of a Landau−Zener rate constant for given R_{AB}, that can span the nonadiabatic to adiabatic limits, was obtained. This expression demonstrates that isotope effects will be more modest than would be expected based on a process where R_{AB} is fixed at the equilibrium separation. For intramolecular hydrogen-atom

TABLE 3: Rate Constants for HAT, Including the Effect of Inner-Sphere Reorganization Energy[a]

ΔG^0 (cm^{-1})	λ_s (cm^{-1})	S_i	Ω_i (cm^{-1})	k (s^{-1})
−2,000	2,000	1.0, 1.0, 1.0, 1.0, 1.0	1500, 2000, 2500, 3000, 3500	1.820×10^8
−2,000	2,000	2.0, 2.0, 2.0, 2.0, 2.0	1500, 2000, 2500, 3000, 3500	1.554×10^6
−1,000	2,000	2.0, 2.0, 2.0, 2.0, 2.0	1500, 2000, 2500, 3000, 3500	5.305×10^5
−3,000	2,000	2.0, 2.0, 2.0, 2.0, 2.0	1500, 2000, 2500, 3000, 3500	3.887×10^6
−1,000	1,000	1.0, 1.0, 1.0, 1.0, 1.0	1500, 2000, 2500, 3000, 3500	1.434×10^8
−1,000	1,000	2.0, 2.0, 2.0, 2.0, 2.0	1500, 2000, 2500, 3000, 3500	1.023×10^6
−2,000	2,000	1.0 (I=0,9)	500+I*250 (I=0,9)	6.019×10^6
−1,000	2,000	1.0 (I=0,9)	500+I*250 (I=0,9)	1.297×10^6
−3,000	2,000	1.0 (I=0,9)	500+I*250 (I=0,9)	1.933×10^7

[a] See eq 5.1 and following for parameter definitions. [b] Without inner-sphere modes $k \sim 1.6 \times 10^{10}$ s^{-1}.

transfers, using typical Lippincott Schroeder potentials and heavy-atom masses and vibrational frequencies. isotope effects of $k_H/k_D \sim 1-6$ were found. For bimolecular processes, where the base and its corresponding acid must climb a repulsive wall to come close enough to react, $k_H/k_D \sim 1-20$. These results are quite sensitive to the details of the potential surfaces, and clearly, the surfaces are rough approximations to the actual surfaces. Nevertheless, the prediction that isotope effects will be smaller than those based on equilibrium-distance transfers should be robust. A greater span in the KIE for the repulsive versus the bonded potential surfaces is anticipated.

If a HAT reaction does have a relatively small isotope effect, then an implication is that the pre-exponential factor in the rate expression will be quite large. This follows from the absence of a small pre-exponential factor from nonadiabatic ET (the V_{el} electronic matrix element) and from the absence of nonadiabatic proton effects that enter as Franck−Condon "drag" factors (cf. eq 2.3). If, in addition, the activation energy is small, HAT reactions will tend to have a large rate constant; the adiabatic limit factor is $\omega_s/2\pi \sim 10^{12}$ s^{-1}. Inclusion of inner-sphere vibrations, appropriate for some HAT reactions, will lead to smaller rate constants, as found experimentally. Of course, with modest activation energies, the rates will already be in the observed range of values.

The kinetic features of a number of HAT reactions can be rationalized on the basis of the above considerations. The data on the reduction of $Y_Z^{\bullet}$,[44,73,74] when expressed in Arrhenius form, $k = A \exp(-E_a/kT)$, is characterized by a range of activation energies, $E_a \sim 1-9$ kcal/mol, small preexponential factors $A \sim 10^6-10^9$ s^{-1} (relative to $A \sim 10^{13}$ s^{-1} for an electron-transfer reaction) and small KIEs, $k_H/k_D \sim 1.3-2.9$. These ranges come from rate measurements particular to various S-state transitions and from different methods of sample preparation. $Y_Z^{\bullet}$ reduction is an excellent candidate for a HAT mechanism, in view of the small donor−acceptor distance. Also, one expects significant changes in equilibrium bond distances in the substrate H_2O manganese cluster upon HAT.[70] The features of relatively low E_a, small isotope effect, and small rate constant (from a small A factor) emerge from the HAT theory for the bonded framework model, with some involvement of inner-sphere vibrations.

In this perspective, $Y_Z^{\bullet}$ reduction is an example of hydrogen-atom transfer between an oxygen atom and an oxy-based radical, and its kinetics should be similar to other oxygen radical transfers. Mahoney and DeRooge[75−77] and Ingold and co-workers[78,79] have studied a large variety of such reactions. They are also characterized by low activation energies, $E_a \sim 1-7$ kcal/mol, log A values of 5−10 M^{-1} s^{-1}, low isotope effects (when measured), and rates $k_{obs} \sim 10^5 - 10^9$ M^{-1} s^{-1}. These bimolecular rate constants can be converted to unimolecular rate constants k_r via $k_{obs} = K_A k_r$ with K_A the association constant, in the limit where the dissociation rate of the encounter complex is fast relative to the atom transfer rate, k_r. For moderately bound encounter complexes that may be anticipated for these systems, $K_A \sim 1$M^{-1},[75−77] unimolecular and bimolecular rates are directly comparable.

Mayer and co-workers[80,81] carefully and systematically examined electron, proton, and hydrogen atom transfer exchange reactions between iron bi-imidazoline complexes, finding an isotope effect of 2.3 for the hydrogen (deuterium) atom exchange. They concluded that the hydrogen atom exchange proceeded as a concerted process. Their data was theoretically analyzed by Iordanova, Decornez, and Hammes-Schiffer[14] with the aim of elucidating PCET/HAT pathways. The relatively long FE donor/acceptor distance places the reaction in the electronically nonadiabatic regime, and the relatively short proton transfer distance leads to good proton wave function overlap and a modest isotope effect. In our scheme, the reaction is a concerted PCET reaction, as we have reserved the term HAT for electronically adiabatic processes.

Mayer and co-workers also emphasize that HAT reaction should have low outer-sphere reorganization energies, λ_s, compared with electron/proton reactions. In constructing the LZ parameter defined in eq 3.10, the λ_s value of 2,000 cm^{-1} was chosen to be relatively small; the smaller it is, the more rapidly with increasing $V_{00}(R_{AB})$ will the proton adiabatic limit be reached. Smaller λ_s values emphasize the small isotope effect limit. If HAT involves minimal charge rearrangement (in contrast with ET and PT), then the reorganization energy arises from "acoustic" (mass displacement) modes of the solvent in response to the atom movement and would be characterized by a Debye frequency $\sim 100-200$ cm^{-1}. Using this order of magnitude for λ_s would decrease the isotope effect substantially. Thus, small isotope effects for HAT for hydrogen-bonded complexes may be a feature of some generality.

The remaining parameter in the LZ factor of eq (3.10) is ω_s the solvent frequency. Recently, Cohen and Huppert[82] studied proton transfer in a protic liquid and found evidence of a transition from nonadiabatic to adiabatic proton transfer as the temperature was decreased. They ascribed this transition to the feature that ω_s increases with increasing temperature. The same transition should be found in HAT.

That rate constants for carbon acids tend to be small, in comparison with oxygen and nitrogen acids, has been noted repeatedly.[52,83] A number of explanations have been put forth that are based on classical transition-state theory arguments. In a classical transition-state theory, the reaction coordinate is a bond-making/breaking coordinate for the transfer atom. By contrast, the theory presented here is designed for light atom tunneling between heavy atoms and invokes the atom coordinate only for the tunneling probability part. The rest of the energetics comes from coupling of the transfer particle to the medium. Thus, the interpretation of activation energy is completely different. In both approaches, the central idea, that carbon acids do not form hydrogen bonds, is invoked to explain why the rates are low, relative to nitrogen and oxygen acids. However, carbon acids tend to exhibit fairly significant isotope effects. Krishtalik[52] pointed out that large isotope effects cannot by explained by classical transition-state theory with corrections for zero point energy effects, necessitating the introduction of a tunneling approach, and noted the role of a repulsive surface in leading to low rates. He also stressed the importance of accounting for the shift in the most probable distance for transfer with isotope. The theory presented here incorporates these effects and does show that a large range of isotope effect should be anticipated for repulsive surfaces. Rates will tend to be low because reaction will be dominated by the large R_{AB} distances, where the proton is in the nonadiabatic regime and the difference in tunneling efficiency between H and D will be enhanced.

We made a number of approximations that provide a relatively simple picture for HAT. Perhaps the most drastic one is that only the ground-state proton levels, in its initial and final states, contribute to the rate constant as in eq 3.8. For reactions where the proton surface before/after electron-transfer tips significantly, as a consequence of having the proton stable in its initial/final state, the dominant contribution to the rate will be from this ground-state-to-ground-state transition. However, there will be additional terms that will modify the rate constant

from higher-order diagonal ($n_i = n_f$) or from off-diagonal contributions ($n_i \neq n_f$). These considerations are for a fixed R_{AB} value. Another approximation, as shown in the Appendix B, permits the rate to be expressed as an average over R_{AB} values. While our development could be used as a starting point of a more general theory, its evaluation would introduce approximations that would be difficult to assess. In view of the uncertainties associated with the various potential energy surfaces that ultimately determine the rate constant's value, one should view this theory as one that has explanatory power for trends, instead of one that will give quantitative estimates for rates. Finally, we have assumed from the outset in constructing our formalism that the electronic transition is adiabatic. In general, the degree of adiabaticity of the proton and electron are related to each other as shown by Georgievskii and Stuchebrukhov.[18] A general theory of PCET will have to account for this coupling.

Appendix A

In this Appendix, we develop an expression for the rate constant of a PCET reaction with inclusion of a heavy-atom framework vibration mode, with coordinate denoted by R_{AB}. It will provide the starting point for the HAT expression that we obtain in section III, using the results of Appendix B.

If we view a PCET reaction from a "double adiabatic" perspective, then the coupling responsible for the charge transfer is

$$V_{etpt} = V_{el}\langle\chi^i_{n_i}|\chi^f_{n_f}\rangle(R_{AB}) \tag{A.1}$$

where, first, the electron and proton fast coordinates are separated from the R_{AB} and solvent slow coordinates, and then the fast-electron coordinate is separated from the proton coordinate.[48] Incorporating this Born−Oppenheimer scheme in a "golden rule" calculation gives the rate-constant expression

$$k = V_{el}{}^2\sum_{j_i}\sum_{n_i}\sum_{\mu_i}P^i_{j_i}\rho^i_{n_i}\rho^i_{\mu_i}\sum_{j_f}\sum_{n_f}\sum_{\mu_f} |\langle\Pi^f_{j_f}|\Pi^i_{j_i}\rangle|^2|\langle\varphi^i_{\mu_i}|\langle\chi^i_{n_i}|\chi^f_{n_f}\rangle(R_{AB})|\varphi^f_{\mu_f}\rangle|^2 \otimes \delta[(E^f_{j_f} - E^i_{j_i}) + (E^f_{\mu_f} - E^i_{\mu_i}) + (\epsilon^f_{n_f} - \epsilon^i_{n_i})] \tag{A.2}$$

The ingredients of eq A.2 are as follows: The energies $E^i_{j_i}(E^f_{j_f})$ and corresponding wave functions $\Pi^i_{j_i}(\Pi^f_{j_f})$ are those of the solvent when the electron and proton are in their initial (final) states. We have neglected the (slight) dependence of these quantities on the specific proton state, $n_i(n_f)$, relative to the major dependence of being in its initial (final) state. The energies $\epsilon^i_{n_i}(\epsilon^f_{n_f})$ and corresponding wave functions $\chi^i_{n_i}(\chi^f_{n_f})$ are those of the proton when the electron and proton are in their initial (final) states. When the solvent fluctuates to an appropriate configuration for charge transfer to occur, the tunnel splitting is given by

$$|\epsilon^f_{n_f} - \epsilon^i_{n_i}| \equiv \Delta\epsilon_{n_in_f} \approx 2\langle\chi^i_{n_i}|\chi^f_{n_f}\rangle(R_{AB})\hbar\sqrt{\omega_i\omega_f} \equiv 2V_{n_in_f}(R_{AB}) \tag{A.3}$$

where $\omega_i(\omega_f)$ are the frequencies in the proton double well when the proton is in its initial (final) state. These matrix elements depend on R_{AB}, as indicated. The connection in eq A.3 between tunnel splittings $\Delta\epsilon_{n_in_f}$ and Franck−Condon factors $\langle\chi^i_{n_i}|\chi^f_{n_f}\rangle$ can be shown by a semiclassical WKB-based procedure.[55] The energies $E^i_{\mu_i}(E^f_{\mu_f})$ and wave functions $\varphi^i_{\mu_i}(R_{AB})(\varphi^f_{\mu_f}(R_{AB}))$ are those characterizing the heavy-atom framework motion when the electron and proton are in their initial (final) states. The matrix elements $\langle\varphi^i_{\mu_i}(R_{AB})|V_{n_in_f}(R_{AB})|\varphi^f_{\mu_f}(R_{AB})\rangle$ represent non-Condon effects for each protonic tunnel splitting $V_{n_in_f}(R_{AB})$. Since the $V_{n_in_f}(R_{AB})$ have a significant R_{AB} dependence on the spatial scale of the $\varphi^i_{\mu_i}(R_{AB})$ and $\varphi^f_{\mu_f}(R_{AB})$ wave functions, these non-Condon effects will be very important. Finally, $P^i_{j_i}$, $\rho^i_{n_i}$, and $\rho^i_{\mu_i}\otimes$ are the equilibrium initial-state distribution functions for, respectively, the solvent orientational polarization, the proton, and the heavy-atom framework vibrational mode.

Two limiting cases that can be obtained from eq A.2 are as follows:

(1) ETPT without non-Condon (R_{AB}) effects. Then we have

$$\langle\varphi^i_{\mu_i}|V_{n_in_f}|\varphi^f_{\mu_f}\rangle = V_{n_in_f}\langle\varphi^i_{\mu_i}|\varphi^f_{\mu_f}\rangle = V_{n_in_f}\delta_{\mu_i\mu_f} \tag{A.4}$$

This assumes that the $\varphi^i_{\mu_i}(R_{AB})$ and $\varphi^f_{\mu_f}(R_{AB})$ are not displaced in the charge-transfer process. If they were, then the R_{AB} mode would make some contribution to the charge-transfer rate via an inner-sphere effect. With eq A.4, eq A.2 becomes

$$k_{etpt} = V_{el}{}^2\sum_{j_i}\sum_{n_i}P^i_{j_i}\rho^i_{n_i}\sum_{j_f}\sum_{n_f}|\langle\Pi^i_{j_i}|\Pi^f_{j_f}\rangle|^2|\langle\chi^i_{n_i}|\chi^f_{n_f}\rangle|^2 \otimes \delta[(E^f_{j_f} - E^i_{j_i}) + (\epsilon^i_{n_i} - \epsilon^f_{n_f})] \tag{A.5}$$

and this is, with the assumption of a classical solvent, what leads to the ETPT rate-constant expression in eq 2.3.[6]

(2) "Pure" PT with non-Condon effects. This is accomplished by keeping only the $n_i = n_f = 0$ term to pick out one proton splitting. And V^2_{el} does not appear for just a proton-transfer reaction, of course. Then, $i(f)$ refer solely to initial (final) proton states. Note that $\rho^i_{n_i} = \delta_{n_i,0}$, since all other proton states are of higher energy. Then

$$k_{pt} = \sum_{j_i}\sum_{\mu_i}P^i_{j_i}\rho^i_{\mu_i}\sum_{j_f}\sum_{\mu_f}|\langle\Pi^i_{j_i}|\Pi^f_{j_f}\rangle|^2 |\langle\varphi^i_{\mu}(R_{AB})|V_{00}(R_{AB})|\varphi^f_{\mu}(R_{AB})\rangle|^2\delta[(E^f_{j_f} - E_{j_ii}) + (E^f_{\mu_f} - E^i_{\mu_i})] \tag{A.6}$$

This expression was the starting point of our Landau−Zener PT theory that can span the nonadiabatic-to-adiabatic PT regimes.[50] Treating the solvent classically then leads to eq 3.1.

Returning to eq A.2 for ETPT with R_{AB} effects included, we set $n_i = n_f = 0$ to obtain

$$k = V_{el}{}^2\sum_{j_i}\sum_{\mu_i}P^i_{j_i}\rho^i_{\mu_i}\sum_{j_f}\sum_{\mu_f}|\langle\Pi^f_{j_f}|\Pi^i_{j_i}\rangle|^2 \otimes |\langle\varphi^i_{\mu_i}(R_{AB})|V_{00}(R_{AB})/\hbar\omega|\varphi^f_{\mu_f}\rangle|^2 \delta[(E^f_{j_f} - E^i_{j_i}) + (E^f_{\mu_f} - E^i_{\mu_i})] \tag{A.7}$$

where we have absorbed $(\epsilon^f_0 - \epsilon^i_0)$ into the definition of the solvation-energy difference $(E^f_{j_f} - E^i_{j_i})$, used eq A.3, and defined $\omega = \sqrt{\omega_i\omega_f}$.

Comparing eq A.7 with the pure PT rate expression of eq A.6 shows that they have the same formal structure. Thus, we can use the same procedure to incorporate adiabaticity effects on the proton dynamics in the case of HAT, as we did for pure PT.

Appendix B

The simplified rate expression in eq 3.9 that is an average over heavy-atom distances is obtained as follows: For a two-mode charge-transfer reaction, where one mode corresponds to

the R_{AB} motion and the other to the hydrogen atom coupled to a (classical solvent), an expression that has a similar formal structure as what we previously obtained for a pure proton transfer can be used[49]

$$k = \frac{\omega_s}{2\pi}\sum_{\mu_i}\rho^i_{\mu_i}\sum_{\mu_f}A(\bar{v}_{00}^{\mu_i\mu_f})\mathrm{e}^{-(\lambda_s+\Delta G^0+E_{\mu f}f-E_{\mu i}i)^2/(4\lambda_s k_B T)} \quad \text{(B.1)}$$

where $A(\bar{v}_{00}^{\mu_i\mu_f})$ is defined in eq 3.5 and the

$$\bar{v}_{00}^{\mu_i\mu_f} \equiv (v_{00}^{\mu_i\mu_f}/v_T) = \frac{2\pi(V_{00}^{\mu_i\mu_f})^2}{\hbar\omega_s\sqrt{2\lambda_s k_B T}} \quad \text{(B.2)}$$

factors are obtained from the matrix elements of the splitting $V_{00}(R_{AB})$, with respect to the R_{AB} wave functions, $\phi_{\mu_i}(R_{AB})$ (not the wave functions of the proton states), according to

$$V_{00}^{\mu_i\mu_f} = \int \mathrm{d}R_{AB}\,\varphi^i_{\mu_i}(R_{AB})V_{00}(R_{AB})\varphi^f_{\mu_f}(R_{AB}) \quad \text{(B.3)}$$

Comparison of eqs 3.1 and 3.8 shows that the identification of $V_{00}^{\mu_i\mu_f}$ (pt) with $V_{el}\Omega_{00}^{\mu_i\mu_f}$ (HAT) provides the desired connection.

The $E^i_{\mu_i}(E^f_{\mu_f})$ (μ_i, μ_f = 0,1,2,...) are the energies in the R_{AB} surface before (after) the atom transfer. We expand $A(\bar{v}_{00}^{\mu_i\mu_f})$ in a power series as

$$A(\bar{v}_{00}^{\mu_i\mu_f}) = \sum_{r=1}a_r(\bar{v}_{00}^{\mu_i\mu_f})^r = \sum_{r=1}c_r(V_{00}^{\mu_i\mu_f}V_{00}^{\mu_i\mu_i})^r \quad \text{(B.4)}$$

where the c_r coefficients are related to the a_r coefficients via eq B.2.

The assumption that the R_{AB} motion does not introduce reorganization energy to the HAT transfer, because the R_{AB} surfaces are minimally displaced in the HAT, reduces eq B.1 to

$$k = \frac{\omega_s}{2\pi}\sum_{r=1}c_r\sum_{\mu_i}\rho^i_{\mu_i}\sum_{\mu_f}(V_{00}^{\mu_i\mu_f}V_{00}^{\mu_i\mu_i})^r\mathrm{e}^{-(\lambda_s+\Delta G^0)^2/4\lambda_s k_B T} \quad \text{(B.5)}$$

To demonstrate that eq B.5 can be written in the R_{AB}-averaged form of eq 3.9, consider the desired general term in its power-series expansion of the R_{AB} matrix element

$$I_{k^{\max}} \equiv \sum_{\mu_i}\rho^i_{\mu_i}\int \mathrm{d}R_{AB}\,\varphi^i_{\mu_i}(R_{AB})V_{00}^{(k^{\max}+1)}(R_{AB})\varphi^i_{\mu_i}(R_{AB}) \quad \text{(B.6)}$$

where $k^{\max} = 1, 3, 5, \ldots$ is an odd integer. We introduce $k^{\max}$ complete sets of states via

$$1 = \int \mathrm{d}R'_{AB}\,\delta(R_{AB}-R'_{AB}) = \int \mathrm{d}R'_{AB}\sum_{\mu_f}\varphi^f_{\mu_f}(R_{AB})\varphi^f_{\mu_f}(R'_{AB}) \quad \text{(B.7)}$$

into the above expression to obtain

$$I_{k^{\max}} = \sum_{\mu}\rho^i_{\mu}[\prod_{k=1}^{k^{\max}}\sum_{\nu_k}V_{00}^{\nu_{k-}1}{}^{\nu_k}]V_{00}{}^{\nu_{k\max}\mu} \quad \text{(B.8)}$$

To simplify the notation, in eq B.8, we set $\mu_i = \mu$, $\mu_f^k = \nu_k$,$\nu_0 = \mu$, and $\nu_1 = \nu$.

Since there is only one pair of levels that cross for a given initial-state surface μ_i in the LZ theory, the state space is restricted to a particular pair of levels. Thus, there is the restriction embodied in the following Kronecker delta functions, $\delta^{(e)}_{\nu_k\mu}$ and $\delta^{(o)}_{\nu_k\nu}$, where (e) denotes that $k = 2, 4, \ldots, k^{\max}-1$ and (o) denotes that $k = 3, 5, \ldots, k^{\max}$. Use of these Kronecker deltas in eq B.8 leads toSetting $r = (k^{\max}+1)/2$ to compare eq B.6

$$\begin{aligned} I_{k^{\max}} &= \sum_{\mu}\rho^i_{\mu}[\prod_{k=1}^{k^{\max}}\sum_{\nu_k}V_{00}^{\nu_{k-}1}\delta\delta^{\nu_k(o)(e)}_{\nu_k\mu\nu_k\nu_1}]V_{00}{}^{\nu_{k\max}\mu} \\ &= \sum_{\mu}\rho^i_{\mu}[\prod_{k=1}^{k^{\max}}\sum_{\nu}V_{00}^{\nu\mu}]V_{00}^{\nu\mu} = \sum_{\mu}\rho^i_{\mu}(V_{00}^{\nu\mu})^{k^{\max}}V_{00}^{\nu\mu} \\ &= \sum_{\mu}\rho^i_{\mu}\sum_{\mu}(V_{00}^{\nu\mu}V_{00}^{\nu\mu})^{(k^{\max}+1)/2} \end{aligned} \quad \text{(B.9)}$$

and B.9 and returning to eq B.5 then yields (with our definition $\mu = \mu_i$)

$$\begin{aligned} k &= \frac{\omega_s}{2\pi}\sum_{r=1}c_r\sum_{\mu}\rho^i_{\mu_i}\int \mathrm{d}R_{AB}\,\varphi^i_{\mu_i}(R_{AB})V_{00}^{2r}(R_{AB})\varphi^i_{\mu_i}(R_{AB})\times \\ &\qquad \mathrm{e}^{-(\lambda_s+\Delta G^0)^2/4\lambda_s k_B T} \\ &= \frac{\omega_s}{2\pi}\sum_{\mu}\rho^i_{\mu_i}\int \mathrm{d}R_{AB}\,|\varphi^i_{\mu_i}(R_{AB})|^2A_{00}(R_{AB})\mathrm{e}^{-(\lambda_s+\Delta G^0)^2/4\lambda_s k_B T} \end{aligned} \quad \text{(B.10)}$$

with

$$\bar{v}_{00}(R_{AB}) \equiv v_{00}(R_{AB})/v_T = 2\pi V_{00}{}^2(R_{AB})/\hbar\omega_s\sqrt{2\lambda_s k_B T} \quad \text{(B.11)}$$

a R_{AB}-dependent LZ parameter that is defined by an analogous power series expression to that given in eq B.4 and 3.5.

Finally, noting that the position representation of the initial state density matrix $P(R_{AB})$ is

$$\sum_{\mu_i}\rho^i_{\mu_i}|\varphi^i_{\mu_i}(R_{AB})|^2 = P(R_{AB}) \quad \text{(B.12)}$$

eq B.10 can be written as

$$\begin{aligned} k &= \frac{\omega_s}{2\pi}\int \mathrm{d}R_{AB}\,P(R_{AB})A_{00}(R_{AB})\mathrm{e}^{-(\lambda_s+\Delta G^0)^2/4\lambda_s k_B T} \\ &= \int \mathrm{d}R_{AB}\,P(R_{AB})k_{00}^{LZ}(R_{AB}) \end{aligned} \quad \text{(B.13)}$$

which is eq 3.9.

Acknowledgment. The financial support of the National Institutes of Health (GM 47274) is gratefully acknowledged.

References and Notes

(1) Krishtalik, L. I. *Adv. Electrochem. Electrochem. Eng.* **1970**, *7*, 283.
(2) Levich, V. G. In *Physical Chemistry - An Advanced Treatise*; Henderson, H., Yost, W., Eds.; Academic: New York, 1970; Vol. 9B, p 985.
(3) Levich, V. G.; Dogonadze, R. R.; German, E. D.; Kuznetsov, A. M.; Kharkats, Y. I. *Electrochim. Acta* **1970**, *15*, 353.
(4) Cukier, R. I. *J. Phys. Chem.* **1994**, *98*, 2377.
(5) Zhao, X. G.; Cukier, R. I. *J. Phys. Chem.* **1995**, *99*, 945.
(6) Cukier, R. I. *J. Phys. Chem.* **1995**, *99*, 16101.
(7) Cukier, R. I. *J. Phys. Chem.* **1996**, *100*, 15428.
(8) Cukier, R.; Nocera, D. *Annu. Rev. Phys. Chem.* **1998**, *49*, 337.
(9) Benderskii, V. A.; Grebenshchikov, S. Y. *J. Electroanal. Chem.* **1994**, *375*, 29.
(10) Fang, J.-Y.; Hammes-Schiffer, S. *J. Chem. Phys.* **1997**, *106*, 8442.
(11) Fang, J.-Y.; Hammes-Schiffer, S. *J. Chem. Phys.* **1997**, *107*, 5727.
(12) Fang, J.-Y.; Hammes-Schiffer, S. *J. Chem. Phys.* **1997**, *107*, 8933.
(13) Decornez, H.; Hammes-Schiffer, S. *J. Phys. Chem. A* **2000**, *104*, 9370.

(14) Iordanova, N.; Decornez, H.; Hammes-Schiffer, S. *J. Am. Chem. Soc.* **2001**, *123*, 3723.
(15) Soudackov, A.; Hammes-Schiffer, S. *J. Chem. Phys.* **2000**, *113*, 2385.
(16) Hammes-Schiffer, S. *Acc. Chem. Res.* **2001**, *34*, 273.
(17) Kuznetsov, A. M.; Ulstrup, J. *Can. J. Chem.* **1999**, *77*, 1085.
(18) Georgievskii, Y.; Stuchebrukhov, A. A. *J. Chem. Phys.* **2000**, *113*, 10438.
(19) Okamura, M. Y.; Feher, G. *Annu. Rev. Biochemistry* **1992**, *31*, 861.
(20) Malmström, B. G. *Acc. Chem. Res.* **1993**, *26*, 332.
(21) Ferguson-Miller, S.; Babcock, G. T. *Chem. Rev.* **1996**, *96*, 2889.
(22) Hoganson, C. W.; Babcock, G. T. *Science* **1997**, *277*, 1953.
(23) Birge, R. R. *Annu. Rev. Phys. Chem.* **1990**, *41*, 683.
(24) Durr, H.; Bouas-Laurent, H. *Photochromism: Molecules and Systems. Studies in Organic Chemistry 40*; Elsevier: Amsterdam, 1990; Vol. 40.
(25) Scherl, M.; Haarer, D.; Fischer, J.; DeCian, A.; Lehn, J.-M.; Eichen, Y. *J. Phys. Chem.* **1996**, *100*, 16175.
(26) Roecker, L.; Meyer, T. J. *J. Am. Chem. Soc.* **1987**, *109*, 746.
(27) Thorp, H. H. *Inorg. Chem.* **1991**, *3*, 171.
(28) Shafirovich, V. Y.; Courtney, S. H.; Ya, N.; Geacintov, N. E. *J. Am. Chem. Soc.* **1995**, *117*, 4920.
(29) Binstead, R. A.; McGuire, M. E.; Dovletoglou, A.; Seok, W. K.; Roecker, L. E.; Meyer, T. J. *J. Am. Chem. Soc.* **1992**, *114*, 173.
(30) Turro, C.; Chang, C. K.; Leroi, G. E.; Cukier, R. I.; Nocera, D. G. *J. Am. Chem. Soc.* **1992**, *114*, 4013.
(31) Kirby, J. P.; Roberts, J. A.; Nocera, D. G. *J. Am. Chem. Soc.* **1997**, *119*, 9230.
(32) Muller, A.; Ratajczaks, H.; Junge, W.; Diemann, E. *Electron and Proton Transfer in Chemistry and Biology*; Elsevier: Amsterdam, 1992.
(33) Holm, R. H.; Solomon, E. I. *Chem. Rev.* **1996**, *96*, 2237.
(34) Kohen, A.; Klinman, J. P. *Acc. Chem. Res.* **1998**, *31*, 397.
(35) Kohen, A.; Klinman, J. P. *Chem. Biol.* **1999**, *6*, R191.
(36) Sutcliffe, M. J.; Scrutton, N. S. *Trends Biochem. Sci.* **2000**, *25*, 405.
(37) Tommos, C.; Babcock, G. T. *Acc. Chem. Res.* **1998**, *31*, 18.
(38) Meyer, B.; Scholddr, E.; Dekker, J. P.; Witt, H. T. *Biochim. Biophys. Acta* **1989**, *974*, 36.
(39) Tommos, C.; Tang, X.-S.; Warncke, K.; Hoganson, C. W.; Styring, S.; McCracken, J.; Diner, B. A.; Babcock, G. T. *J. Am. Chem. Soc.* **1995**, *117*, 10325.
(40) Chu, H.-A.; Nguyen, A. P.; Debus, R. *Biochemistry* **1995**, *34*, 5839.
(41) Westphal, K. L.; Tommos, C.; Cukier, R. I.; Babcock, G. T. *Curr. Opin. Plant Biol.* **2000**, *3*, 236.
(42) Yocum, C. F.; Pecoraro, V. L. *Curr. Opin. Struct. Biol.* **1993**, *3*, 182.
(43) Barber, J.; Kuhlbrandt, W. *Curr. Opin. Struct. Biol.* **1999**, *9*, 469.
(44) Tommos, C.; Babcock, G. T. *Biochim. Biophys. Acta* **2000**, *1458*, 199.
(45) Landau, L. D. *Phys. A. Sowjetunion* **1932**, *2*, 46.
(46) Zener, C. *Proc. R. Soc. London, Ser. A* **1932**, *37*, 696.
(47) Nikitin, E. E.; Umanskii, S. Y. *Theory of Slow Atomic Collisions*; Springer-Verlag: Berlin, 1984.
(48) Ulstrup, J. *Charge-Transfer Processes in Condensed Media*; Springer: Berlin, 1979.
(49) Borgis, D.; Hynes, J. T. *J. Phys. Chem.* **1996**, *100*, 1118.
(50) Cukier, R. I.; Zhu, J. *J. Phys. Chem. B* **1997**, *101*, 7180.
(51) Bell, R. P. *The Tunnel Effect in Chemistry*; Chapman and Hall: London, 1980.
(52) Krishtalik, L. I. *Charge-Transfer Reactions in Electrochemical and Chemical Processes*; Plenum: New York, 1979.
(53) Marcus, R. A. *Annu. Rev. Phys. Chem.* **1964**, *15*, 155.
(54) Marcus, R. A.; Sutin, N. *Biochim. Biophys. Acta* **1985**, *811*, 265.
(55) Fain, B. *Lecture Notes in Chemistry: Theory of Rate Processes in Condensed Media*; Springer-Verlag: Berlin/Heidelberg, 1980.
(56) Lippincott, E. R.; Schroeder, R. *J. Chem. Phys.* **1955**, *23*, 1099.
(57) Gilli, P.; Bertolasi, V.; Ferretti, V.; Gilli, G. *J. Am. Chem. Soc.* **1994**, *116*, 909.
(58) Vener, M. V. *Chem. Phys. Lett.* **1995**, *244*, 89.
(59) Scheiner, S. In *Proton Transfer in Hydrogen-Bonded Systems*; Bountis, T., Ed.; Plenum: New York, 1992; Vol. 291, p 29.
(60) Zeeger-Huyskens, T.; Huyskens, P. In *Proton Transfer and Ion Transfer Complexes*; Ratajczak, H., Orville-Thomas, W. J., Eds.; Wiley: New York, 1980; Vol. 2, p 1.
(61) Benderskii, V. A.; Goldanski, V. I.; Ovchinnikov, A. A. *Chem. Phys. Lett.* **1980**, *73*, 492.
(62) Benderskii, V. A.; Goldanski, V. I.; Makarov, D. E. *Phys. Rep.* **1993**, *233*, 195.
(63) Borgis, D.; Lee, S.; Hynes, J. T. *Chem. Phys. Lett.* **1989**, *162*, 19.
(64) Morillo, M.; Cukier, R. I. *J. Chem. Phys.* **1990**, *92*, 4833.
(65) Suárez, A.; Silbey, R. *J. Chem. Phys.* **1991**, *94*, 4809.
(66) Borgis, D.; Hynes, J. T. *Chem. Phys.* **1993**, *170*, 315.
(67) Borgis, D.; Hynes, J. T. *J. Chem. Phys.* **1991**, *94*, 3619.
(68) Staib, A.; Borgis, D.; Hynes, J. T. *J. Chem. Phys.* **1995**, *102*, 2487.
(69) Zavitsas, A. A.; Chatgilialoglu, C. *J. Am. Chem. Soc.* **1995**, *117*, 10645.
(70) Blomberg, M. R. A.; Siegbahn, P. E. M.; Styring, S.; Babcock, G. T.; Åkermark, B.; Korall, P. *J. Am. Chem. Soc.* **1997**, *119*, 8285.
(71) Kubo, R.; Toyozawa, Y. *Prog. Theor. Phys.* **1955**, *13*, 160.
(72) Kestner, N. R.; Jortner, J.; Logan, J. *J. Phys. Chem.* **1974**, *78*, 2148.
(73) Tommos, C.; Hoganson, C. W.; DiValentin, M.; Lydakis-Simantiris, N.; Dorlet, P.; Westphal, K.; Chu, H.-A.; McCracken, J.; Babcock, G. T. *Curr. Opin. Chem. Biol.* **1998**, *2*, 244.
(74) Karge, M.; Irrgang, K. D.; Renger, G. *Biochemistry* **1997**, *36*, 8904.
(75) Mahoney, L. R.; DaRooge, M. A. *J. Am. Chem. Soc.* **1975**, *97*, 4722.
(76) Mahoney, L. R.; DaRooge, M. A. *J. Am. Chem. Soc.* **1972**, *94*, 7002.
(77) Mahoney, L. R.; DaRooge, M. A. *J. Am. Chem. Soc.* **1969**, *92*, 890.
(78) Foti, M.; Ingold, K. U.; Lusztyk, J. *J. Am. Chem. Soc.* **1994**, *116*, 9440.
(79) Evans, C.; Scaiano, J. C.; Ingold, K. U. *J. Am. Chem. Soc.* **1992**, *114*, 4589.
(80) Roth, J. P.; Lovell, S.; Mayer, J. M. *J. Am. Chem. Soc.* **2000**, *122*, 5486.
(81) Mayer, J. M. *Acc. Chem. Res.* **1998**, *31*, 441.
(82) Cohen, B.; Huppert, D. *J. Phys. Chem. A* **2001**, *105*, 2980.
(83) Bender, M. L. *Mechanisms of Homogeneous Catalysis from Protons to Proteins*; John Wiley & Sons: New York, 1971.